

A GENERATIVE MODEL FOR HALLUCINATING DIVERSE VERSIONS OF SUPER RESOLUTION IMAGES

Mohamed Abid, Ihsen Hedhli, Christian Gagné*

IID, Université Laval, *Canada-CIFAR AI Chair, Mila

ABSTRACT

Traditionally, the main focus of image super-resolution techniques is on recovering the most likely high-quality images from low-quality images, using a one-to-one low- to high-resolution mapping. Proceeding that way, we ignore the fact that there are generally many valid versions of high-resolution images that map to a given low-resolution image. We are tackling in this work the problem of obtaining different high-resolution versions from the same low-resolution image using Generative Adversarial Models. Our learning approach makes use of high frequencies available in the training high-resolution images for preserving and exploring in an unsupervised manner the structural information available within these images. Experimental results on the CelebA dataset confirm the effectiveness of the proposed method, which allows the generation of both realistic and diverse high-resolution images from low-resolution images.

Index Terms— Super-resolution, Image Hallucination, Generative Adversarial Models.

1. INTRODUCTION

Image super-resolution (SR) is an ill-posed problem, since each low-resolution (LR) image can have a practically infinite number of corresponding images in the high-resolution (HR) domain. However, traditional SR techniques rely on a one-to-one schema, aiming at generating (or reconstructing) only one HR image from a LR image, generally the most likely one. However, they still do not account for all other possible mappings. In practice, in applications such as microscopy or medical imaging, where experts rely on SR methods, having access to more than one possible solution can lead to better strategies where different outcomes, and even the certainty on these outcomes, are considered.

In this paper, we seek to perform a one-to-many schema by generating a diverse set of HR images out of one single LR image. For that, we are proposing to use a Generative Adversarial Network (GAN) that recovers an HR image from a very LR version of the same image, meanwhile being able to hallucinate a wide variety of other acceptable HR versions of this image. In the recent literature, some exploratory SR has been investigated, for example relying on SR methods that

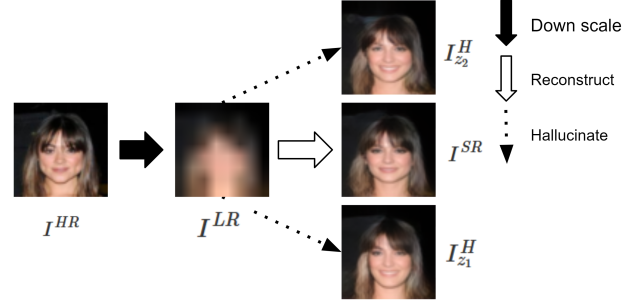


Fig. 1. Conceptual representation of proposed approach: starting from an original image (I^{HR}) and its downsampled version (I^{LR}), different HR images can be generated, that is here the reconstructed image (I^{SR}) and two hallucinated ones ($I_{z_1}^H$ and $I_{z_2}^H$).

are either controlled by a user interface to manually manipulate the variance and periodicity of textures [1], or by using semantically guided style imposition [2]. The diversity generated in these methods are supervised, by either a human or a specific criterion, which is in contrast to our method where hallucination is conducted in an unsupervised way. Another approach such as [3] searches in a pretrained GAN’s manifold for a set of high-resolution images that maps, when down-scaled, to the same low-resolution image. While this method yields great quality samples, it is an iterative procedure that requires a significant amount of time to generate each image. Meanwhile our method is a one pass-prediction which works for general images and is not dependent on a pretrained GAN (e.g., StyleGAN).

Methods such as [4] exploited the image’s gradient as structure guidance for super-resolution. This helps the model to better learn and preserve structural and textural information in the image. We follow a similar path but we are not limiting its use to preserve the structure of the image but to anchor the exploration over the image-gradient manifold in order to generate other images that would preserve most of the structure given by the image’s gradient. The main contribution of the paper lies in the novel neural architecture that makes use of high-frequency within the image not only to recover one HR image but also to generate a wide variety of plausible HR im-

ages that downscale to the same LR version of of this image – see Fig. 1 that illustrates the concept of our approach.

2. APPROACH

Given a LR image I^{LR} , the objective of the proposed approach is twofold:

- Reconstruct the ground truth HR image that allows the retrieval of its corresponding image gradient;
- Hallucinate a variety of HR images that match, when downscaled, the input LR image (I^{LR}).

To tackle the aforementioned objectives, we propose a generator G that takes as input pairs of (I^{LR}, z) , where z is a m -dimensional white noise vector, $z \sim \mathcal{N}^m(0, 1)$. We follow the same assumptions made in [5], with our proposed model deemed to reconstruct the ground-truth HR image when $z = 0$, otherwise ($z \neq 0$) sampling a variety of images matching the LR input but having a varied image gradient:

$$G(I^{LR}, 0) = (I^{SR}, g^{SR}) \quad (\text{reconstruction}), \quad (1)$$

$$G(I^{LR}, z) = (I_z^H, g_z^H) \quad (\text{hallucination}). \quad (2)$$

In these equations, I^{SR} is the reconstructed ground-truth image while I_z^H is a hallucinated version given a noise vector z . Also, g^{SR} and g_z^H are respectively the reconstructed image gradient of the ground truth image and the hallucinated image gradient given a noise vector z .

2.1. Image Reconstruction

Like traditional SR models, the proposed model aims to minimize the distance between the ground-truth and the reconstructed HR images. In addition, our model aims to preserve structural information in the original image by using the ground-truth image I^{HR} and its correspond gradient g^{HR} , computed as follows:

$$g_x = I^{HR}(x+1, y) - I^{HR}(x-1, y), \quad (3)$$

$$g_y = I^{HR}(x, y+1) - I^{HR}(x, y-1), \quad (4)$$

$$g^{HR} = \|(g_x, g_y)\|_2. \quad (5)$$

As shown in (1), the generator takes as input the pair $(I^{LR}, 0)$ and outputs (I^{SR}, g^{SR}) . The Perceptual loss [6] with VGG-16 [7] is then used by comparing the obtained I^{SR} to the real I^{HR} , by minimizing the Euclidean distances between the features of these images:

$$\mathcal{L}_{percp} = \mathbb{E}_{I^{SR}} \|\phi_i(I^{SR}) - \phi_i(I^{HR})\|_1, \quad (6)$$

where ϕ_i is value output by the i -th layer of VGG. As for comparing the gradient images, the mean absolute error of the images (pixels) is used:

$$\mathcal{L}_{grad} = \|g^{SR} - g^{HR}\|_1. \quad (7)$$

Finally, for both domains, we use an adversarial loss for assessing the quality of the images and gradients generated, that is a non-saturating logistic loss [8] with R_1 regularization [9].

2.2. Image Hallucination

Unlike the reconstruction, image hallucination does not rely on comparing the generated image to the ground truth image. Now in addition to the low-resolution input image I^{LR} , the proposed method uses a random vector z to generate and explore other plausible solutions. However, it is worth noting that conditional GANs (cGANs) suffer from mode collapse problems [10, 11]. Also cGANs tend to ignore the random vector z when conditioned on inputs that contain significant information about the output, for example in image-to-image translation models [12, 13] where the model tends to ignore the random vector. Without addressing this problem in cGANs, the hallucinated images would be equal to the reconstructed image and the model will regress to the same behaviour of one-to-one mapping. To circumvent this problem, we impose on the model a diversity constraint first introduced in [14], which is applied here only on the gradient output, to orient exploration of the structural and texture space of the gradient image.

To enforce the effect of z for obtaining diverse solutions, the generator aims at maximizing loss $\mathcal{L}_z(G)$:

$$\mathcal{L}_z(G) = \mathbb{E}_{z_1, z_2 \sim \mathcal{N}^n(0, 1)} \left[\min \left(\frac{d(g_{z_1}^H, g_{z_2}^H)}{\|z_1 - z_2\|}, \tau \right) \right], \quad (8)$$

where $d(\cdot, \cdot)$ is a distance metric, and $g_{z_1}^H$ and $g_{z_2}^H$ are the gradient images obtained from HR hallucinated images with z_1 and z_2 sampled from $\mathcal{N}^n(0, 1)$, respectively, both hallucinated images obtained from the same LR input. The minimum with τ is conducted to ensure numerical stability of the optimization, in case where the output is not bounded by an activation function (e.g., tanh or sigmoid).

Maximizing $\mathcal{L}_z(G)$ encourages the generator to explore more the HR space, by producing a varied set of hallucinated samples. To make sure that the hallucinated samples stay faithful to the given LR input image, we impose the following constraint:

$$\|\text{DS}(I_z^H) - I^{LR}\| < \epsilon, \quad (9)$$

where $\text{DS}(\cdot)$ is a down-scaling operation, and ϵ is a hyper-parameter.

2.3. Overall Objective

Two discriminators are used in the generative model, one for assessing the HR images (D_I) and the other to validate its corresponding gradient (D_g). For both networks, non-saturating logistic loss [8] with R_1 regularization [9] is used:

$$\begin{aligned} \mathcal{L}_{adv}^g &= -\mathbb{E}_{g^{HR}} [\log(1 - D_g(g^{HR}))] - \mathbb{E}_{g^{SR}} [\log D_g(g^{SR})], \\ \mathcal{L}_{adv}^I &= -\mathbb{E}_{I^{HR}} [\log(1 - D_I(I^{HR}))] - \mathbb{E}_{I^{SR}} [\log D_I(I^{SR})]. \end{aligned}$$

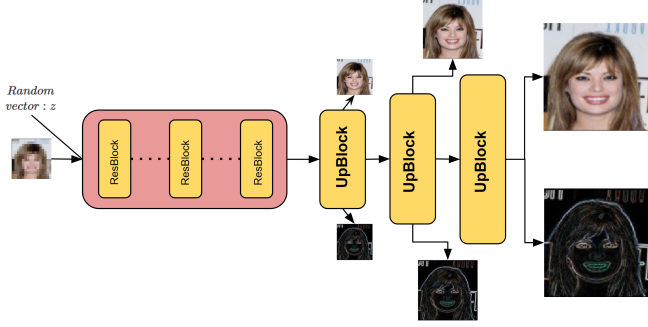


Fig. 2. Generator Architecture: the network consists of 8 residual blocks followed by stacked upsampling blocks (Up-blocks) – see Fig. 3 for the inner layers of UpBlock.

As for generating reconstructed HR images, we use a weighted sum over \mathcal{L}_{percp} (6), \mathcal{L}_{grad} (7) and the adversarial loss:

$$\mathcal{L}_{recons} = \gamma(\mathcal{L}_{percp} + \mathcal{L}_{grad}) + \beta(\mathcal{L}_{adv}^g + \mathcal{L}_{adv}^I). \quad (10)$$

And for generating hallucinated HR images, the loss is:

$$\mathcal{L}_{halluc} = \mathcal{L}_{adv}^g + \mathcal{L}_{adv}^I + \alpha\mathcal{L}_z. \quad (11)$$

3. IMPLEMENTATION

3.1. Conditioning

We choose to condition the discriminator D_I on the constraint (9) by concatenating it at the last block of the network. We follow [5] by rounding the downscaled fake image to the closest colour value and dividing it by $r = 2/255$ (since images are in the range $[-1, 1]$).

$$F = \max \left(\left(\frac{||DS(I_z^H) - I^{LR}||}{r} - \epsilon, 0 \right) \right). \quad (12)$$

That prevents producing exceedingly large values for the discriminator’s weights in order to measure infinitesimal differences. A straight through estimator is used to pass the back-propagation gradient through the rounding operation. Therefore, the discriminator receives two inputs, fake/real images and F given in (12):

$$\begin{cases} D_I(I^{HR}, 0) & \text{for real images} \\ D_I(I_z^H, F) & \text{for fake images} \end{cases}.$$

3.2. Architecture

Our model consists of a generator, that takes a LR image, a noise vector, and outputs two images: a HR image and its corresponding gradients. Two discriminators are also used during the learning, which are taking real/fake images and their gradients, respectively.

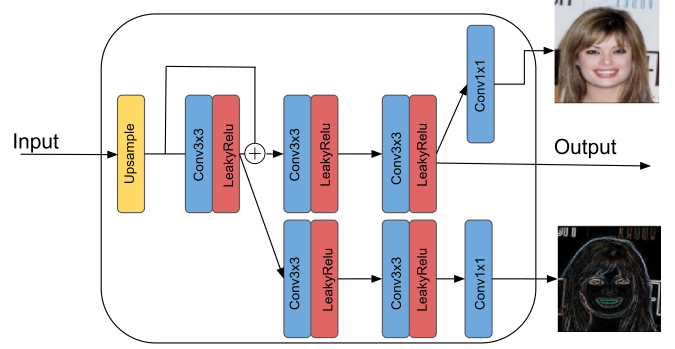


Fig. 3. Upblock architecture: a convolution block shared between the two domains is used to enable the learning of image structures, which are then followed by two domain-specific convolution and a 1×1 convolution to make a projection of the values in the feature space into the pixel space. The key in using a skip connection is to keep the low frequency information such as colours intact.

The generator global architecture is inspired by [15] (see Fig. 2). First the residual blocks take the LR image with noise vectors, then they are followed by up-sampling blocks, where each block outputs an image and its corresponding gradient at that scale (see Fig. 3). This way the gradient flows to the generator at different scales, allowing it to be more stable, leading to a faster learning. As mentioned before, two discriminators are used, one for each domain (I^{HR} and g^{HR}), their architecture is mirrored version of the generator, but since each discriminator is domain-specific, the upblock is replaced by a downblock, where we use first a 1×1 convolution to pass the image from the pixel space to feature space. This is followed by another two convolutions, by leaky RELUs and then by average pooling for downsampling. After the downsampling blocks, the residual blocks are just like the generator. The discriminator directly outputs the features of last convolutions, without using linear layers.

4. EXPERIMENTS

4.1. Settings

Experiments were conducted on the CelebA [16] dataset, to assess the capability of our model, which was trained on up-scaling images 8 times and then compared to other SR methods (i.e., [17] and [18]).

Our model is trained with the Adam optimizer[19] ($lr = 1e^{-4}$, $\beta_1 = 0.$, $\beta_2 = 0.9$) with TTUR [20], using batch sizes equal to 8. We use a leaky RELU for all activation functions in the generator and both discriminators, with a leak equal to 0.2.

We fix ϵ in (12) to 0.1, while for \mathcal{L}_{recons} we set $\gamma = 10$ and $\beta = 0.1$, and for \mathcal{L}_{halluc} , α is equal to 1.

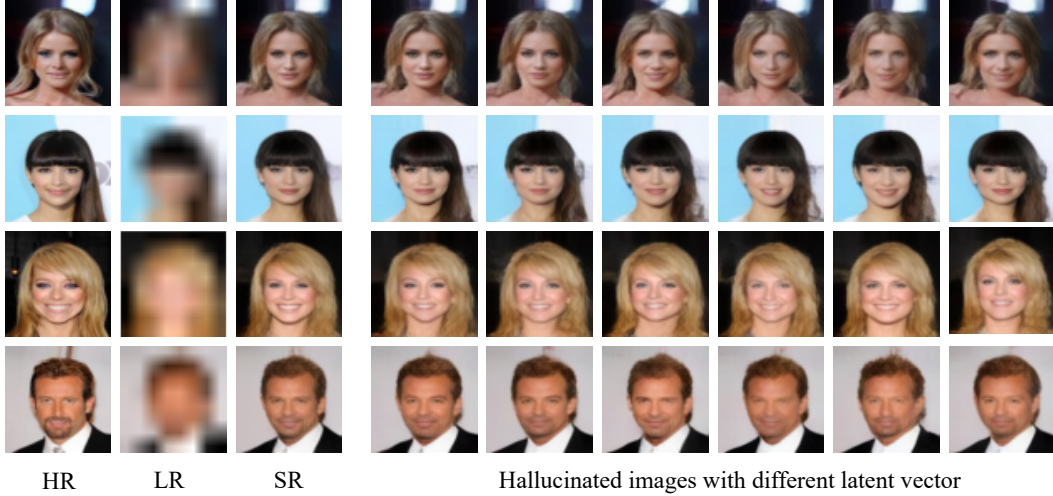


Fig. 4. Results on 8x scaling: reconstruction (SR) and hallucination using different z vectors

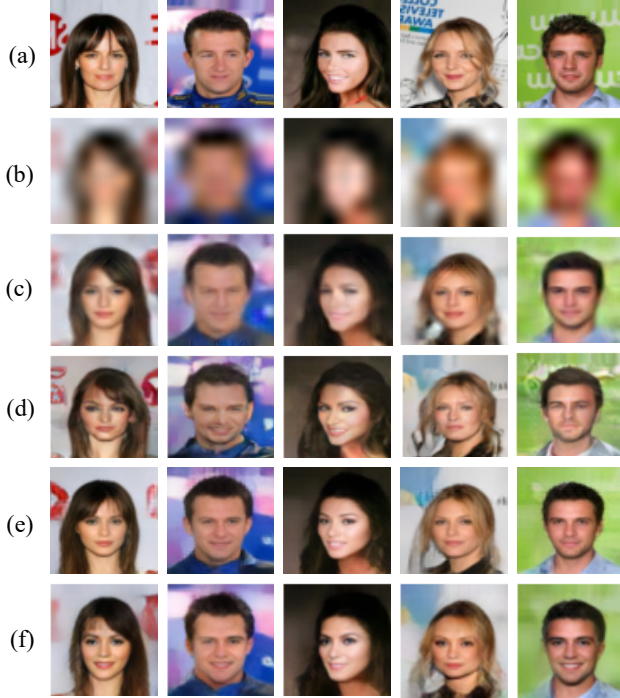


Fig. 5. Results on CelebA 8x scaling: (a) ground truth, (b) bicubic reconstruction, (c) SRGAN, (d) Esrgan, (e) Ours : Reconstruction ($z = 0$), and (f) Ours : Hallucination ($z \neq 0$).

4.2. Results

We use the traditional SR metrics peak signal-to-noise ratio (PSNR), structural similarity index (SSIM) and learned perceptual image patch similarity (LPIPS) [21]. Although our method is optimized to generate images with high perceptual quality, which means that the results do not correlate very well with PSNR and SSIM [21], we still achieve excellent perfor-

Method	SSIM \uparrow	PSNR \uparrow	LPIPS \downarrow
Bicubic	0.43	18.11	0.51
SRGAN [17]	0.62	20.15	0.24
ESRGAN [18]	0.55	18.43	0.23
Ours	0.68	21.08	0.18

Table 1. Comparison of results for 8x scaling on CelebA [16], all results are reported on the test set.

mance, with an improvement by a large margin on all metrics – see Table 1 for details.

We report the results of our model and compare these results with the results obtained using the approaches described in [17, 18]. We show that when the input is a very low resolution image, where most of the information is missing, the use of the gradient has a huge impact on the results. As illustrated in Fig. 5, the reconstructions of our model are closer to the real images than other methods, but also more coherent since the structural properties of the images is being preserved by making the model learn the gradient of the image.

In addition to having better reconstruction given the use of $\epsilon = 0.1$ for (9) in our experiments, the model has more freedom to hallucinate other semantics that do not appear in the low-resolution image, such as changing the facial expressions or even changing the person’s identity (see Fig. 4).

5. CONCLUSION

In this paper we propose a new super-resolution method that makes use of novel GAN architecture that is able to recover images from extremely low resolution images, and hallucinate a wide variety of other possibilities. We showed the superiority of our approach in both tasks on the CelebA dataset.

6. REFERENCES

- [1] Yuval Bahat and Tomer Michaeli, “Explorable Super Resolution,” *arXiv e-prints*, p. arXiv:1912.01839, Dec. 2019.
- [2] Marcel Christoph Bühler, A. Romero, and R. Timofte, “Deepsee: Deep disentangled semantic explorative extreme super-resolution,” *ArXiv*, vol. abs/2004.04433, 2020.
- [3] Sachit Menon, Alexandru Damian, Shijia Hu, Nikhil Ravi, and Cynthia Rudin, “PULSE: Self-Supervised Photo Upsampling via Latent Space Exploration of Generative Models,” *arXiv e-prints*, p. arXiv:2003.03808, Mar. 2020.
- [4] Cheng Ma, Yongming Rao, Yean Cheng, Ce Chen, Jiwu Lu, and Jie Zhou, “Structure-Preserving Super Resolution with Gradient Guidance,” *arXiv e-prints*, p. arXiv:2003.13081, Mar. 2020.
- [5] David Berthelot, Peyman Milanfar, and Ian Goodfellow, “Creating High Resolution Images with a Latent Adversarial Generator,” *arXiv e-prints*, p. arXiv:2003.02365, Mar. 2020.
- [6] Justin Johnson, Alexandre Alahi, and Fei-Fei Li, “Perceptual losses for real-time style transfer and super-resolution,” *CoRR*, vol. abs/1603.08155, 2016.
- [7] Karen Simonyan and Andrew Zisserman, “Very deep convolutional networks for large-scale image recognition,” in *3rd International Conference on Learning Representations, ICLR 2015, San Diego, CA, USA, May 7-9, 2015, Conference Track Proceedings*, Yoshua Bengio and Yann LeCun, Eds., 2015.
- [8] Ian Goodfellow, Jean Pouget-Abadie, Mehdi Mirza, Bing Xu, David Warde-Farley, Sherjil Ozair, Aaron Courville, and Yoshua Bengio, “Generative adversarial nets,” in *Advances in Neural Information Processing Systems*, Z. Ghahramani, M. Welling, C. Cortes, N. Lawrence, and K. Q. Weinberger, Eds. 2014, vol. 27, pp. 2672–2680, Curran Associates, Inc.
- [9] Lars M. Mescheder, “On the convergence properties of GAN training,” *CoRR*, vol. abs/1801.04406, 2018.
- [10] Tim Salimans, Ian J. Goodfellow, Wojciech Zaremba, Vicki Cheung, Alec Radford, and Xi Chen, “Improved techniques for training gans,” *CoRR*, vol. abs/1606.03498, 2016.
- [11] Martin Arjovsky and Léon Bottou, “Towards Principled Methods for Training Generative Adversarial Networks,” *arXiv e-prints*, p. arXiv:1701.04862, Jan. 2017.
- [12] Phillip Isola, Jun-Yan Zhu, Tinghui Zhou, and Alexei A. Efros, “Image-to-image translation with conditional adversarial networks,” *CoRR*, vol. abs/1611.07004, 2016.
- [13] Jun-Yan Zhu, Taesung Park, Phillip Isola, and Alexei A. Efros, “Unpaired image-to-image translation using cycle-consistent adversarial networks,” *CoRR*, vol. abs/1703.10593, 2017.
- [14] Dingdong Yang, Seunghoon Hong, Yunseok Jang, Tianchen Zhao, and Honglak Lee, “Diversity-sensitive conditional generative adversarial networks,” *CoRR*, vol. abs/1901.09024, 2019.
- [15] Animesh Karnewar, Oliver Wang, and Raghu Seshu Iyengar, “MSG-GAN: multi-scale gradient GAN for stable image synthesis,” *CoRR*, vol. abs/1903.06048, 2019.
- [16] Ziwei Liu, Ping Luo, Xiaogang Wang, and Xiaoou Tang, “Deep learning face attributes in the wild,” in *Proceedings of International Conference on Computer Vision (ICCV)*, December 2015.
- [17] Christian Ledig, Lucas Theis, Ferenc Huszar, Jose Caballero, Andrew P. Aitken, Alykhan Tejani, Johannes Totz, Zehan Wang, and Wenzhe Shi, “Photo-realistic single image super-resolution using a generative adversarial network,” *CoRR*, vol. abs/1609.04802, 2016.
- [18] Xintao Wang, Ke Yu, Shixiang Wu, Jinjin Gu, Yihao Liu, Chao Dong, Chen Change Loy, Yu Qiao, and Xiaoou Tang, “ESRGAN: enhanced super-resolution generative adversarial networks,” *CoRR*, vol. abs/1809.00219, 2018.
- [19] Diederik P. Kingma and Jimmy Ba, “Adam: A method for stochastic optimization,” in *3rd International Conference on Learning Representations, ICLR 2015, San Diego, CA, USA, May 7-9, 2015, Conference Track Proceedings*, Yoshua Bengio and Yann LeCun, Eds., 2015.
- [20] Martin Heusel, Hubert Ramsauer, Thomas Unterthiner, Bernhard Nessler, Günter Klambauer, and Sepp Hochreiter, “Gans trained by a two time-scale update rule converge to a nash equilibrium,” *CoRR*, vol. abs/1706.08500, 2017.
- [21] Richard Zhang, Phillip Isola, Alexei A. Efros, Eli Shechtman, and Oliver Wang, “The unreasonable effectiveness of deep features as a perceptual metric,” *CoRR*, vol. abs/1801.03924, 2018.